

# Low-Cost Satellite Attitude Control Sensors Based on Integrated Infrared Detector Arrays

A. W. van Herwaarden

**Abstract**—This paper describes attitude control systems (ACS) for satellites and a new, static system based on an integrated infrared (IR) detector array. After a short introduction on the use and control of satellites in general, we explain the advantage of static systems, made possible by the use of integrated IR detector arrays. In particular, the static system is lighter and smaller than the previous systems, and requires less power. The electronics is updated to state-of-the-art, increasing the autonomy of the system and thereby reducing its dependence upon the satellite microcontroller.

The detectors are based on a bipolar silicon process for the mechanical structure (using electrochemically controlled etching (ECE)-potassium hydroxide (KOH) etching), with an SiN membrane for thermal isolation of the pixels, which have a polymer black coating for transduction of radiation to heat and n-type versus p-type polysilicon thermopiles for heat detection. The pixel pitch is  $600\ \mu\text{m}$ , the black area is approximately  $495 \times 440\ \mu\text{m}^2$ , and the pixel sensitivity is approximately  $55\ \text{V/W}$ , at a thermopile resistance of  $23\ \text{k}\Omega$ . Two types of detectors have been designed: a single-array type with 32 pixels in two staggered arrays, and a chip with four 32-pixel arrays integrated in a cross. This has made it possible to make a family of earth sensors for the different missions in space.

**Index Terms**—Earth sensor, infrared (IR) array, infrared (IR) detector, satellite.

## I. INTRODUCTION

**T**HERE is an increasing use of satellites orbiting the earth for many applications. Originally used for espionage purposes, many dozens of satellites (sometimes even working in team effort) are now responsible for weather surveillance, communication and TV signal relay, agriculture monitoring, highly accurate positioning systems (GPS), and satellite-mobile-phone systems. These satellites in an earth-bound orbit need attitude control systems (ACS) for a correct orientation of the platform with respect to the earth. In this way, antennas will be properly oriented onto relay stations on Earth and cameras will monitor the desired portion of the earth's surface.

The increased use of such satellites is an incentive to develop new, cost-efficient instruments. The cost-efficiency is found not only in cheaper parts and assembly of the instrument, but also in better functionality and lower mass and size.

## II. ATTITUDE CONTROL OF SATELLITE PLATFORMS

The attitude control of a spacecraft makes use of sensors that measure the instantaneous directions of fields emitted by the surrounding celestial bodies: magnetic field, gravity gradient,

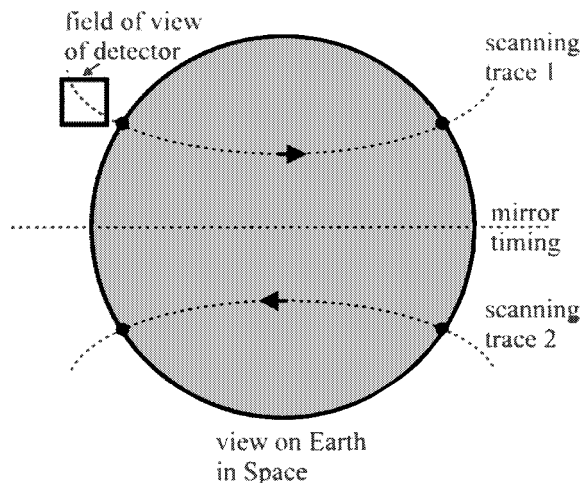


Fig. 1. In the single-element detector earth sensor a rotating mirror projects a trace of Earth on the detector, enabling it to determine the space–earth transitions with respect to the earth sensor.

and optical radiation. Optical instruments are used for accurate applications, and for earth-orbiting satellites two types of optical sensors are mainly used: star tracker and earth sensor [1], [2]. The star tracker is an optical camera which images a star pattern on the focal plane of a charge-coupled device (CCD) matrix array, and which can very accurately determine the orientation of the satellite in a Galilean reference coordinate system. The earth sensor is a thermal device which determines the edges of the infrared (IR) earth in the  $14\text{--}16\ \mu\text{m}$  wavelength band, and by doing this keeps the sensor (and thus the platform) exactly oriented toward the earth (centered or biased) with respect to the orbital reference coordinate system.

The earth sensor is generally less accurate than a star tracker, but more tolerant to space radiation and also much less costly. Therefore, it is very widely used for various types of ACS, especially for geostationary platforms where the required lifetime is the longest.

Present models of earth sensors are based on a single-element IR detector which scans the earth thanks to a rotating or oscillating mirror [1]. The mirror makes the detector scan a trace on Earth, so that it first crosses the space–earth transition in the northwest, and then the earth–space transition in the northeast (see Fig. 1). These transitions are measured by the detector in the  $14\text{--}16\ \mu\text{m}$  band, in which Earth has a much higher emission than space and which is not affected by day–night and season variations. The same then happens for the southern hemisphere. The exact location (in the reference frame of the earth sensor) is determined by comparing the transition moments with the mirror position timing.

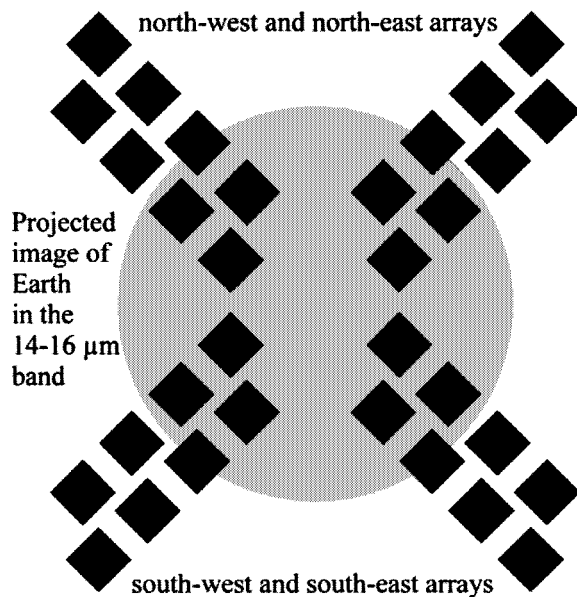


Fig. 2. In the static earth sensor STS02, four IR detector arrays of 32 pixels each (shown schematically) view the image of the earth and determine its exact orientation with respect to the static earth sensor, without using moving parts.

Sodern in France (a subsidiary of EADS), a renowned manufacturer of both star trackers and earth sensors, has developed a new generation of earth sensors without moving parts. This has led to the static earth sensor, which is more compact, smaller, lighter and more economic than earth sensors which use rotating or oscillating mirrors [1]–[3]. In addition, it presents also advantages in terms of longer lifetime, higher reliability, and better instrument autonomy.

The basic idea of the new generation of static earth sensors is to replace the single detector plus rotating mirror by four static arrays of IR detectors. They continuously look at the northwest, northeast, southwest, and southeast edges of Earth, thus removing the need for scanning. With arrays of 32 elements each a good resolution of the space–earth transition can be obtained while maintaining a wide field of view, necessary to acquire Earth during launch or any other transfer orbit type. The configuration of the static earth sensor then becomes as in Fig. 2.

Each array consists of 32 pixels (elements) which are arranged in two staggered arrays of 16 pixels next to each other. Staggered means that the arrays are shifted half a pixel length with respect to each other, and the effect of this is that there is always one pixel which has a full view of the space–earth transition. These arrays are called in-line staggered arrays (ISA); Fig. 3 shows a photograph of the ISA together with multiplexer electronics.

For satellites in low earth orbit (LEO) or medium earth orbit (MEO), the edges of Earth are on four opposite sides of the earth sensor instrument because the satellite is flying so low over Earth. In earth sensors for LEO and MEO applications, four separate germanium lenses are used to project the IR image of the edges onto four separate ISA detector arrays.

For a satellite in a geostationary orbit (GEO), the IR image of the entire earth is projected onto the detector by means of one single lens. In order to maximize the dynamic range of the earth sensor (i.e., the ratio between highest and lowest altitude of the

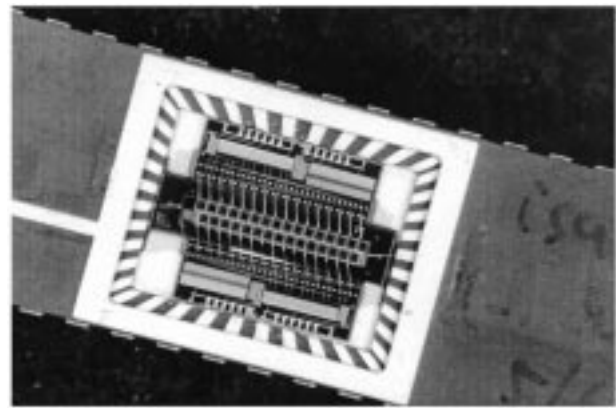


Fig. 3. Photograph of the ISA silicon IR chip (size  $13.5 \times 4 \text{ mm}^2$ ) containing a  $2 \times 16$  staggered array of IR pixels to detect the edge of Earth in the 14–16  $\mu\text{m}$  band, with two CMOS radiation-hard multiplexers.

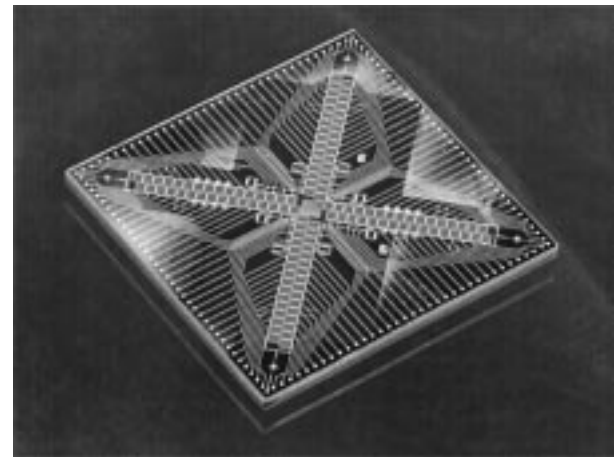


Fig. 4. Photograph of a FPA silicon IR detector chip (size  $20.5 \times 20.5 \text{ mm}^2$ ) integrating four ISA arrays for GEO applications.

satellite where the earth sensor can still view the edge of Earth), it is necessary to minimize the blind area in the center of the four detectors. By integrating the four ISA arrays in one chip, the blind spot in the middle can be reduced further than by using four separate array chips. This led to the design and fabrication of the focal plane array (FPA) detector [4], shown in Fig. 4.

This chip has a dynamic range of about  $10\times$ , allowing operation from 15 000 km up to 140 000 km altitude. Such an operating range is required because of the varying altitude of the satellite during the transfer orbit. The static earth sensor brings a reduction in size, weight and power consumption of a factor of 2–3, compared to the present-day rotating-mirror earth sensor. This is also due to the very compact size of the FPA chip, which enabled Sodern to scale-down the entire design of the earth sensor. Fig. 5 shows the entire static earth sensor, which is approximately  $13 \times 14 \times 15 \text{ cm}^3$  large. In Fig. 5, the bottom part is occupied by three layers of electronics: the analog electronics on top (closest to the detector, which is in the heart of the instrument), the digital electronics in the middle, and the power and communication electronics at the bottom. Each board has connectors to the outside. Above the detector unit, the housing of the germanium lens can be seen, which is shaped to ward off stray radiation. Because the earth sensor will detect the earth with an



Fig. 5. Photograph of the static earth sensor STS02 for geostationary applications incorporating the FPA detector chip.

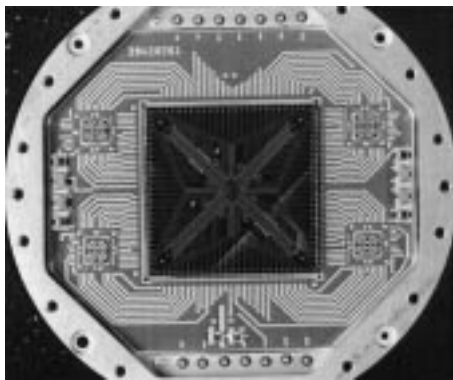


Fig. 6. The MCM, consisting of the FPA detector chip mounted in a ceramic hybrid with radiation resistant multiplexers inside a metal suspension ring.

accuracy of better than  $0.1^\circ$ , a high degree of mechanical stability and proper mounting options are required, and therefore a special housing has been developed for the entire instrument.

### III. EARTH-SENSOR SYSTEM DESIGN

Sodern has designed the system with a flexible concept in mind. Using only different detectors and lenses in an otherwise standard instrument reduces cost of development and production and increases reliability. The major improvements achieved with the development of the new series of earth sensors for LEO, MEO, and GEO were

- a lower mass by a factor of 3;
- a lower power consumption by a factor of 2;
- a better reliability due to the absence of moving parts (particularly a problem in space vacuum);
- an improved lifetime of up to 20 y in GEO;
- a greater autonomy.

These improvements were made possible mainly by using the new detector concept of IR arrays and a cross of arrays. The difference in field of view between LEO and GEO and orbits in between made it necessary to use two concepts: one with a single lens and detector chip and one with four lenses and four separate detectors. For both concepts, a multichip module (MCM) is made. The GEO version contains the chip with the four detector arrays, combined with four radiation-hard multiplexers,

one for each array, see Fig. 6. The other versions contain two or four separate MCMs consisting of a single array with a single multiplexer.

The signals coming off the MCM in a multiplexed mode are then further processed. To correctly calculate the orientation of the earth sensor is carried out in the following steps [2]:

- pixel signal amplification and filtering, 14-bit AD conversion and correction with a factory-determined calibration constant;
- calculation of the earth/space transition for each array from the pixel data;
- calculation of the roll and pitch angles (attitude with respect to Earth).

These actions are performed by an ASIC and a space-qualified microprocessor from Harris, and additional electronics managing the bus communication and power supply. Three small boards are stacked performing the analog/digital functions, communications functions and the power supply function, respectively. They are at the bottom of the housing (see Fig. 5, which also shows the connectors to the three boards). The MCM is located above the boards, with the lens assembly on top of it all. The lens is made of germanium, and has a  $40^\circ$  field of view. For the LEO sensors, which feature separate lenses for each detector arrays, the field of view is only  $22^\circ$ . The main system characteristics are given in Table I.

### IV. FABRICTION OF THE DETECTOR

In this section, we describe the fabrication and design of the basic pixel, the ISA, and the FPA. Fabrication is listed first, since the fabrication technology at hand determines the input for the modeling and design. Staggered arrays of IR detectors have been fabricated before (see, for example, [5]). They achieved a high pixel density with a high sensitivity by bulk etching of one long membrane accommodating all pixels. A low crosstalk was attained with silicon separation beams between the individual pixels. Other devices use front micromachining with arrays or matrices of bolometers, which can also be very sensitive in vacuum applications. However, we deal with ultralow signals (tens of microvolts only). A detector based on thermopiles with their inherent offsetless character is more convenient when going to 128 elements, than the bolometers that Sodern used in its single-element models, with their high offset and obligatory biasing circuitry, which also require thermal regulation and periodic calibration. Therefore, the choice of sensing element fell upon a thermopile-based sensor.

At the University of Michigan, Baer *et al.* obtained the silicon separation beams by a high p-type dose deposition ( $5 \times 10^{19} \text{ cm}^{-3}$ ), which prevents the silicon from being etched during micromachining [5]. The DIMES-process used for this device is a silicon-silicon nitride technology [6], in which n-type epilayer beams in a p-type environment are preserved using electrochemically controlled etching (ECE) in potassium hydroxide (KOH) [6]. Fig. 7 shows one of these beams as it has been etched out from the silicon substrate, the silicon-nitride membrane visible underneath. Visible to the left and the right of the silicon beam are polysilicon thermocouples and the absorbing areas of two neighboring pixels of the array (the aluminum back plate for

TABLE I  
MAIN CHARACTERISTICS OF THE STATIC EARTH SENSOR

Parameter	Value	Unit	Model
Update frequency	4	Hz	all
Accuracy	0.100	degrees	4-lense/ISA (LEO)
	0.035	degrees	1 lense/FPA (GEO)
Mass	1.1	kg	GEO
Size	145×125×140	mm <sup>3</sup>	GEO
Power consumption	3.5	W	
Start-up time	5	sec	

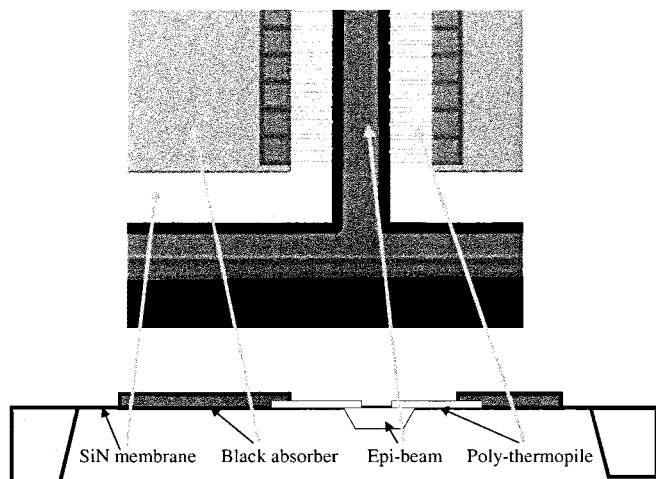


Fig. 7. Photograph from the back side of the chip. Details visible are the silicon beam etched out from the substrate for thermal isolation between IR pixels the aluminum back plates for temperature equalization, and the polysilicon thermocouples.

temperature equalization, and some thin black lines showing the black absorber where the aluminum is left out).

The process we thus chose consisted of a standard bipolar or CMOS part, with lay-out measures and technology additions to enable KOH-ECE etching. The lay-out details include aluminum interconnection between the separate die in the sawing lane, with contacts openings to the epi-layer (locally doped for proper contact), and an aluminum contact area of typically 1 cm<sup>2</sup> for electrical contact to the gold spring-loaded contact of the etching holder. Another measure is the removal of aluminum on the wafer edge. The bipolar/CMOS steps are used to create a mechanical structure, a thin-film add-on module is used to fabricate the silicon–nitride (low-stress) membrane and the p-type versus n-type polysilicon thermopiles [7]. The process closely resembles that described in [6], with the addition of a second metal layer because of the complexity of the interconnection. An in-house black layer process is used to blacken the pixels and make them sensitive to IR radiation in the 14–16 μm band. This process yields a robust polymer black layer, which is scratch resistant and can be patterned using standard IC technology steps. This allows handling of the wafer after deposition of the black layer.

## V. MODELING

We have modeled the required pixel and some possible array configurations in two manners, to obtain results for different pa-

rameters, and also to cross-check the validity of our modeling. On the one hand, we have used a simple discrete-element model allowing us to get an idea of sensitivity and time constant, and we used an EXCEL sheet to perform these calculations. We have also used ANSYS 5.3 for a FEM modeling, to arrive at the optimum configuration for the pixel design for parameters such as sensitivity and crosstalk. For this, we set up a two-dimensional model, since the detectors will be operated in vacuum, and no heat losses through air are present, and radiation losses can be neglected. A square-mesh model was used, each pixel was divided into squares of 15 × 15 μm<sup>2</sup> or 25 × 25 μm<sup>2</sup>, giving the exact temperature on the two sides of thermopiles, the hot and cold side. The size of the mesh depended on the size of the thermopile, which was generally taken to be 30 μm or 50 μm long. The width of the thermopile is of the order of 500 μm. In the modeling, we used the following thermal conductivity values (low-stress SiN ≈ 3 W/Km, mono-Si ≈ 150, poly-Si ≈ 30, aluminum ≈ 200, oxide ≈ 1.5), and a Seebeck coefficient of 230 μV/K for the polysilicon. The ANSYS modeling has been based on a six-pixel part of the array, one pixel being irradiated by Earth, the other five not. In this way, we have established the sensitivity of an irradiated pixel, by dividing the calculated temperature difference versus input radiation power, and we have determined the crosstalk. In particular, Sodern wanted to optimize the quality factor for the pixels [8], given by

$$QF = AS/(\sigma_d^2 + \sigma_e^2)^{0.5} \text{ m}^2 \text{ Hz}^{1/2} \text{ W}^{-1}$$

where  $A$  is the active area of the pixel in m<sup>2</sup> (prescribed by Sodern),  $S$  is the pixel sensitivity in V/W,  $\sigma_d^2$  is the square of the detector noise ( $\approx 4kTR$ ) and  $\sigma_e^2$  is the same for the electronics,  $\sigma_e < 20 \text{ nV}/\sqrt{\text{Hz}}$ . The  $QF$  was eventually optimized to above 500 m<sup>2</sup> Hz<sup>1/2</sup> W<sup>-1</sup>. For this optimization, we have varied the size of the silicon–nitride membrane, varied the sizes of the silicon beams used to thermally separate the pixels, and varied the thermopile length (typically 30–50 μm) and the black absorber area. The black absorber area was mainly determined by the specifications of Sodern. The width of the silicon beams separating the pixels was increased until satisfactory suppression of the crosstalk was obtained. The thermopile and nitride membrane geometry were varied until an acceptable  $QF$  was reached.

The value of  $QF$  has been calculated both with EXCEL models (based on discrete element, each pixels being composed of a capacitance and two or three thermal resistances) and with the ANSYS model.

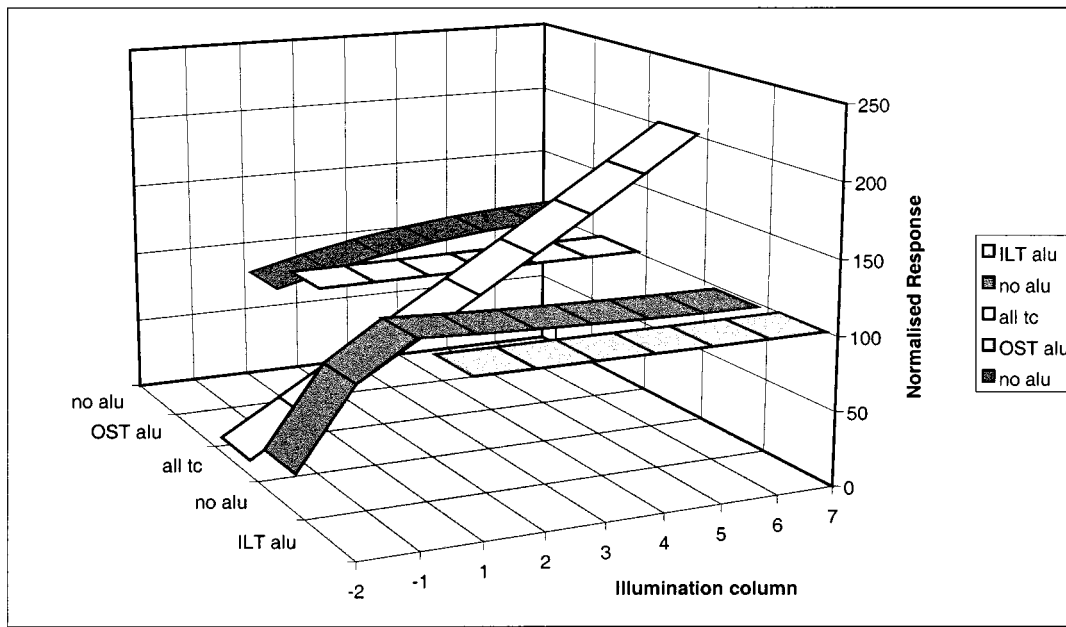


Fig. 8. Graphical output of EXCEL on the modeling of a pixel for various configurations with or without aluminum back plate, showing the improvement in temperature homogeneity due to the aluminum back plate. Shown is the response of five different sensor designs (in the y-axis) for illumination in any one of the six columns of  $25 \mu\text{m}$  width (in the x-axis). The OST (structure with thermopiles perpendicular to the array axis) and the ILT (structure with the thermopile in line with the array axis, as in the ISA and FPA devices fabricated later on) give similar results on temperature homogeneity with aluminum back plates. Without aluminum back plate, there is some inhomogeneity in response, which is different for the different designs.

TABLE II  
MAIN CHARACTERISTICS OF ISA/FPA CHIP

Parameter	Design value	Experimental Value	Unit
Chip size ISA	as small as possible	13.5× 4.0	mm
Chip size FPA		20.5×20.5	
Pixel pitch	600	600	$\mu\text{m}$
Active area	495×440	495×440	$\mu\text{m}$
Poly-Silicon thickness		300	nm
P-type poly sheet resist		75	$\Omega/\text{sq}$
N-type poly sheet resist		50	$\Omega/\text{sq}$
Pixel resistance	<15	23.5	k $\Omega$
Temperature Coefficient of resistance		-0.1	%/K
Uniformity of resistance		<4	%
Sensitivity (in vacuum)	>50	55	V/W
Temperature Coefficient of sensitivity	<0.25	+0.2	%/K
Uniformity of sensitivity	<10	<10	%
Time constant	<16	<10	ms
Radiation tolerance	100	>400	krad

Fig. 8 shows an example of the graphical output from EXCEL (numerical output has been acquired as well), where the device is divided into six columns with absorber, and two columns nitride membrane. Fig. 8 clearly shows the improvement in the temperature homogeneity which is accomplished by using an aluminum back plate underneath the black area. This can be seen in the front calculation (ILT alu) and the second calculation from the back (OST alu), which show very flat response as

function of position. A very long thermopile (all tc) and the two simulations without aluminum back plate (no alu) give different forms of a nonflat response.

The design targets and the values measured on manufactured devices are given in Table II. Only the electrical resistance is slightly higher than originally intended, but in combination with the electronics processing the detector signals, this turned out to be permissible.

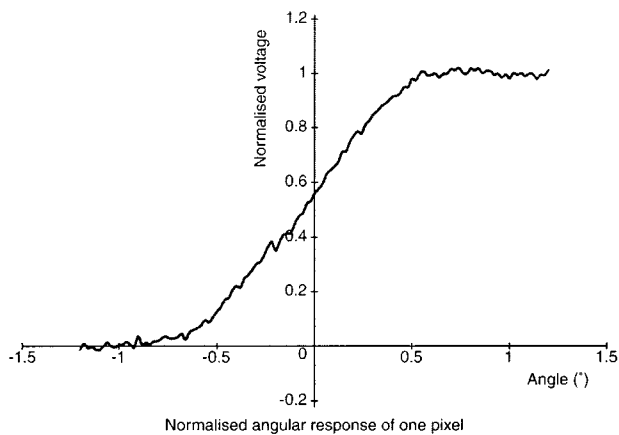


Fig. 9. Normalized angular response of one pixel.

## VI. REDESIGN CONSIDERATIONS

The modeling led to a few different alternatives which were then fabricated and measured [4]. In particular, we tried two different designs with a single array of 32 pixels and one with two staggered arrays of 16 pixels (called ISA). The single arrays have the disadvantage of blind areas, but the design with staggered arrays does not have this disadvantage, and was chosen for the subsequent developments. These were fabricated in the standard DIMES CMOS process with the addition of the thin-film thermopiles and the ECE-KOH provisions. The batch also included CMOS multiplexers with a design that was made radiation hard by surrounding all transistor gates by guard rings and making a spacious design (see Fig. 3).

The ISA detectors made in the first batch showed that some minor process adjustments were needed to arrive at the proper geometry and electrical resistance of the pixels. This was done in the second batch, which yielded satisfactory ISA arrays. The multiplexers fabricated in the first batch performed as designed. They successfully withstood several hundred kRad of radiation, demonstrating their radiation hardness in space. However, Sodern wanted to go into the direction of the FPA concept, with four ISA detectors on one chip. The size of this FPA design, which was eventually squeezed into  $20.5 \times 20.5 \text{ mm}^2$ , required a complicated lithographic processing. Therefore, the concept of combining the FPA and multiplexers on a single chip was abandoned.

Instead, the FPA chip is mounted in a ceramic hybrid with the multiplexers around it (see Fig. 6), in a special metal ring for suspension in the earth sensor instrument (the MCM).

## VII. EXPERIMENTAL RESULTS

Extensive measurements have been made on the ISA devices, including measurements of their radiation hardness. As might be expected, radiation is not a problem for devices such as these,

which electrically consist of active layers (polysilicon and aluminum) separated by dielectric layers (silicon dioxide and nitride).

The measured values for some characteristic parameters are listed in Table II, together with the design targets. This shows that the chips fully function as originally intended, with the only compromise in a slightly higher pixel resistance. However, by keeping the spread in pixel resistance low, this is acceptable.

Fig. 9 shows the normalized output of a pixel when the earth-space transition is moving across the absorbing area. After compensation by software of distortions, a linearity error of less than  $0.025^\circ$  remains. This enables Sodern to achieve the overall earth sensor accuracy of  $0.035^\circ$ .

## VIII. CONCLUSION

A new generation of earth sensors have been developed, instruments for accurately aligning satellites with Earth, based on novel IR detector arrays. Both single ISA with 32 pixels and FPA with four ISA-arrays in a cross have been designed and fabricated. After initial modeling and fabrication of test designs, an optimized array was eventually designed and fabricated meeting all the major requirements and confirming the modeling results.

The chips, which integrate one (ISA) or four (FPA) IR detector arrays on a single die, allow the fabrication of earth sensors without any moving parts, with a twofold to threefold reduction of size, weight (3.3 kg–1.1 kg), and power consumption (7.5 W–3.5 W).

## REFERENCES

- [1] O. Brunel and J. P. Krebs, "Flight results of a new GEO infrared earth sensor STD 15 on board TC2," *AAS 93-324*, pp. 1–15, 1993.
- [2] J. P. Krebs, L. Blarre, G. Coste, and D. Vilaire, "A new family of low cost attitude control sensors," in *Proc. 49th Int. Astronautical Congress*, Melbourne, Australia, Sept. 28–Oct. 2 1998, IAF-98-U.5.06.
- [3] J. P. Krebs and R. Navoni, "New static earth sensor STS02 for GEO platforms," in *Int. Workshop Spacecraft Attitude and Orbit Control Systems*. Noordwijk, The Netherlands: ESTEC, Sept. 15–17, 1997.
- [4] A. W. van Herwaarden, F. G. van Herwaarden, S. A. Molenaar, B. Goudena, M. Laros, P. M. Sarro, C. A. Schot, W. van der Vlist, L. Blarre, and J. P. Krebs, "Fabrication of a focal plane array infrared detector for a satellite attitude control system," in *Proc. Transducers*, Sendai, Japan, June 7–10, 1999, 2D3.1.
- [5] W. G. Baer, K. Najafi, K. D. Wise, and R. S. Toth, "A 32-element micro-machined thermal imager with on-chip multiplexing," *Sens. Actuators A*, vol. A48, pp. 47–54, 1995.
- [6] P. M. Sarro, A. W. van Herwaarden, and W. van der Vlist, "A silicon–silicon nitride fabrication process for smart thermal sensors," *Sens. Actuators A*, vol. 42, pp. 666–671, 1994.
- [7] P. M. Sarro, "Sensor technology strategy in silicon," *Sens. Actuators A*, vol. 31, pp. 138–143, 1992.
- [8] J. P. Krebs, L. Blarre, and D. Guillon, "Low cost static infrared earth sensors for small and microsatellites in LEO," in *Proc. 4th Int. Symp. Small Satellites Systems and Services*, Sept. 14–18, 1998.

A. W. van Herwaarden, photograph and biography not available at the time of publication.